SUPPLEMENTAL FIGURES AND LEGENDS

Figure S1. Genome-wide reorganization of chromosomes and active gene promoters in GCB-cells (related to Figure 1). **A**, Restriction digest of a representative ligation amplicon between neighboring HindIII DNA fragments in Hi-C and 3C control DNA templates. Ligation amplicons were not detected in Hi-C and 3C DNA templates generated with non-cross-linked, purified genomic NB and GCB-cell DNA (data not shown). 3C control ligation amplicons are digested by HindIII but not by NheI. Hi-C ligation amplicons are digested by NheI but not by HindIII, confirming successful restriction site fill-in and ligation of sequenced Hi-C DNA libraries. **B**, Plots showing an inverse relationship between interaction frequency and genomic distance for all filtered intra-chromosomal interactions in sequenced Hi-C libraries from NB and GCB-cells. **C**, Hierarchical cluster dendrogram showing reproducibility between intra-chromosomal interactions in NB and GCB-cell Hi-C biological replicates, with distances expressed as 1–correlation. **D**, (Left) Light microscopy images of Wright-Giemsa-stained NB and GCB-cells showing relative nuclear size. Scale bars represent 10 μm. (Right) Quantification of the relative sizes of the nuclear diameters of Wright-giemsa-stained NB and GCB-cells (n=50; unpaired t-test). **E**, Plot showing the numbers of Hi-C interactions connecting 1 Mb blocks of DNA that were significantly different between GCB and NB-cells (FDR=0.05; Fisher's exact test with BH correction). Numbers of interactions that were gained (84,684) or lost (50,472) in GCB-cells are plotted per chromosome. **F**, Correlation between enrichment of active (H3K4me3, H3K4me2, H3K27Ac) but not repressive (H3K27me3) chromatin marks and normalized interaction frequencies (%) at promoters in GCB-cells. Median enrichment levels were compared between the 25% most interactive promoters and all other quartiles, using non-parametric Wilcoxon tests. **G**, UCSC Genome Browser tracks showing normalized interaction frequencies for NB and GCB-cells at genes with higher promoter interactivity in GCB-cells. Red arrow denotes the start and direction of transcription. Green shading indicates the promoter regions analyzed (TSS±2Kb). **H**, Transcript levels of the genes in (f) as determined by RNA-seq in NB and GCB-cells. **I**, GSEA heat-map showing enrichment (red) or depletion (blue) of gene sets in rank-ordered lists of highly interactive promoters (genes >20 Kb in size) in NB and GCB-cells (FDR=0.10). Non-significant values are indicated in black. Gene sets are ranked by FDR value and their size (n) is indicated. Gene sets were obtained from a curated database (see Supplementary Methods). **J**, Correlations between normalized interaction frequencies and levels of factor binding, as determined by ChIP-chip or ChIP-seq at gene promoters in NB-cells or B-cell lines (compared to all promoters). Significance was determined using Mann-Whitney's test.

Figure S1

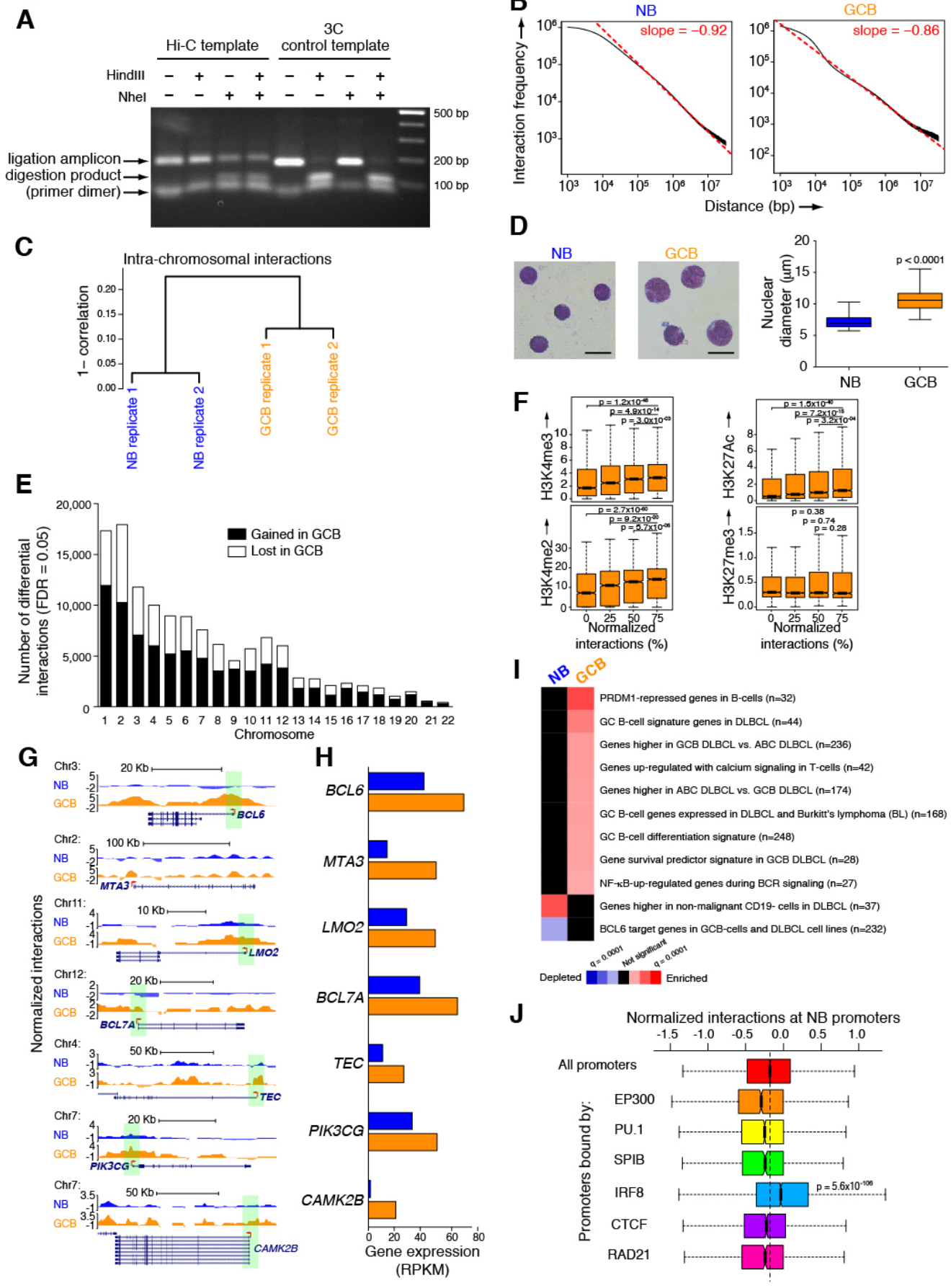
A
Hi-C template
3C control template
HindIII
NheI
500 bp
200 bp
100 bp
ligation amplicon
digestion product
(primer dimer)
B
NB
GCB
slope = −0.92
slope = −0.86
Interaction frequency
Distance (bp)
C
Intra-chromosomal interactions
1 − correlation
NB replicate 1
NB replicate 2
GCB replicate 1
GCB replicate 2
D
NB
GCB
Nuclear diameter (μm)
p < 0.0001
E
Gained in GCB
Lost in GCB
Number of differential interactions (FDR = 0.05)
Chromosome
F
H3K4me3
H3K27Ac
H3K4me2
H3K27me3
Normalized interactions (%)
G
Normalized interactions
BCL6
MTA3
LMO2
BCL7A
TEC
PIK3CG
CAMK2B
H
Gene expression (RPKM)
I
PRDM1-repressed genes in B-cells (n=32)
GC B-cell signature genes in DLBCL (n=44)
Genes higher in GCB DLBCL vs. ABC DLBCL (n=236)
Genes up-regulated with calcium signaling in T-cells (n=42)
Genes higher in ABC DLBCL vs. GCB DLBCL (n=174)
GC B-cell genes expressed in DLBCL and Burkitt's lymphoma (BL) (n=168)
GC B-cell differentiation signature (n=248)
Gene survival predictor signature in GCB DLBCL (n=28)
NF-κB-up-regulated genes during BCR signaling (n=27)
Genes higher in non-malignant CD19- cells in DLBCL (n=37)
BCL6 target genes in GCB-cells and DLBCL cell lines (n=232)
Depleted
Not significant
Enriched
J
Normalized interactions at NB promoters
All promoters
Promoters bound by:
EP300
PU.1
SPIB
IRF8
CTCF
RAD21

Figure S2. Enhancer-promoter interactions are enriched in GCB-cells (related to Figure 2).
A, Correlation between normalized interaction frequency and enhancer regions (H3K4me2pos H3K4me3neg) in NB and GCB-cells compared to the genome. ***p<10-300; Mann-Whitney's test. **B**, Ratio of enhancer-promoter interactions (left panel) and normalized expression (log2 ratio, right panel) of genes with higher enhancer-promoter interactivity in GCB-cells (FDR=0.05). Genes are ranked by significance. Dotted line represents a fold change of 1. **C**, The *CKS2* gene promoter is looped with two distal enhancer regions in GCB-cells. UCSC Genome Browser tracks showing histone marks across the CKS2 gene region, in NB and GCB-cells, where H3K4me3neg H3K4me2pos and H3K27Acpos mark active enhancer regions (enhancer 1 and 2), and locations of genes. Arrows indicate 3C primers (anchor in red). 3C enrichment (n=3), as measured by the 3C assay, was averaged across the regions indicated. *p<0.1; one-tailed, unpaired t-test.

Figure S2

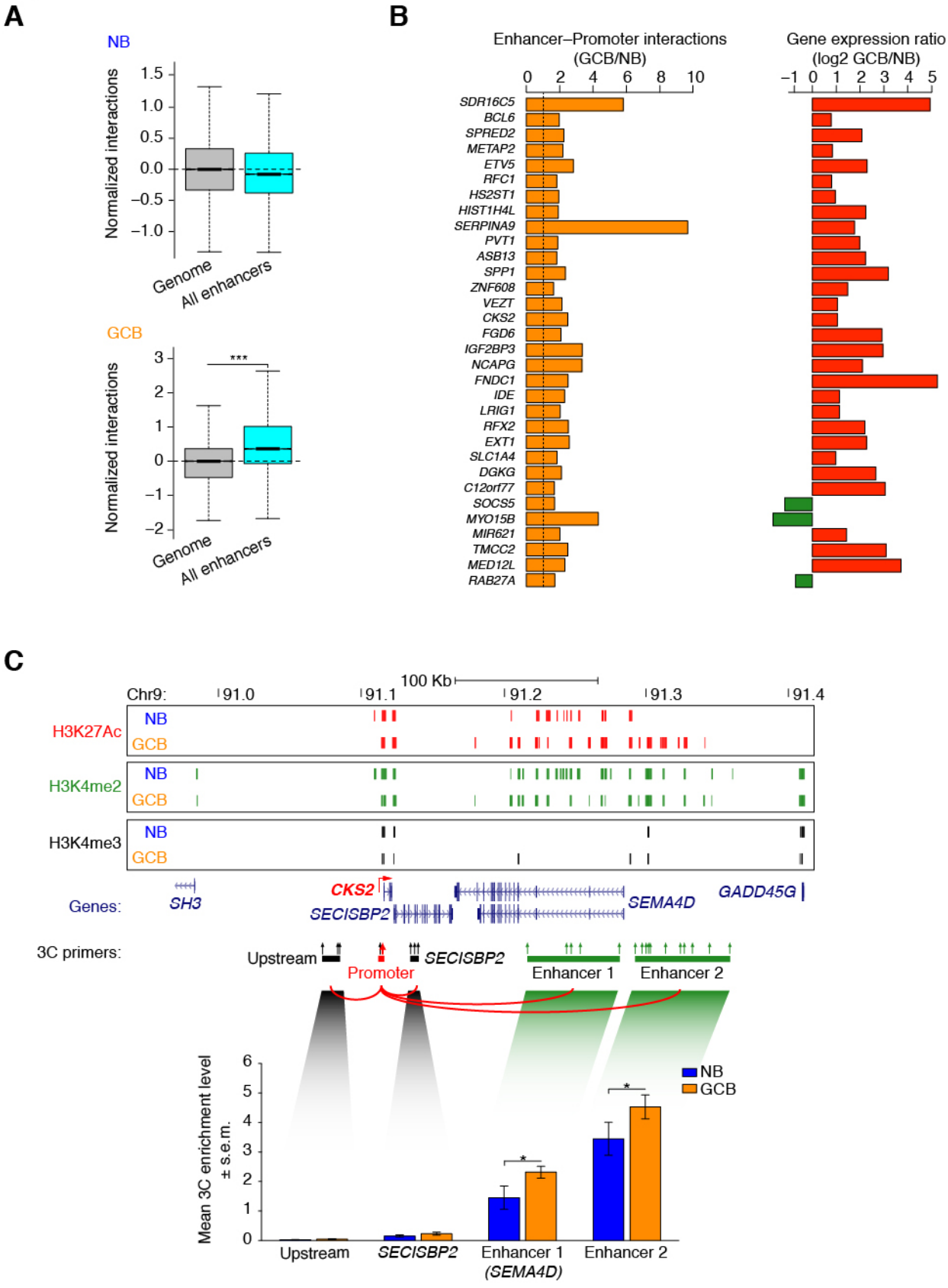
A
NB
Normalized interactions
1.5
1.0
0.5
0.0
−0.5
−1.0
Genome
All enhancers
GCB
***
3
2
1
0
−1
−2
B
Enhancer–Promoter interactions
(GCB/NB)
0 2 4 6 8 10
Gene expression ratio
(log2 GCB/NB)
−1 0 1 2 3 4 5
SDR16C5
BCL6
SPRED2
METAP2
ETV5
RFC1
HS2ST1
HIST1H4L
SERPINA9
PVT1
ASB13
SPP1
ZNF608
VEZT
CKS2
FGD6
IGF2BP3
NCAPG
FNDC1
IDE
LRIG1
RFX2
EXT1
SLC1A4
DGKG
C12orf77
SOCS5
MYO15B
MIR621
TMCC2
MED12L
RAB27A
C
Chr9:
91.0
91.1
100 Kb
91.2
91.3
91.4
H3K27Ac
H3K4me2
H3K4me3
NB
GCB
Genes:
SH3
CKS2
SECISBP2
SEMA4D
GADD45G
3C primers:
Upstream
Promoter
SECISBP2
Enhancer 1
Enhancer 2
Mean 3C enrichment level
± s.e.m.
6
5
4
3
2
1
0
*
*
NB
GCB
Upstream
SECISBP2
Enhancer 1
(SEMA4D)
Enhancer 2

Figure S3. Formation of gene loops in GCB-cells is associated with activated gene expression and CTCF and RAD21 binding (related to Figure 3).

A, Ratio of 5' to 3' gene looping (left panel) and expression of genes (log2 ratio, right panel) with increased looping in GCB-cells (FDR=0.05). Genes are ranked by significance. Dotted line represents a fold change of 1. **B**, Average enrichment of active (H3K4me3, H3K4me2, H3K27Ac) and repressive (H3K27me3) chromatin marks at genes with increased (+) or decreased (–) gene looping in GCB-cells. Chromatin mark enrichment was determined for the gene body and for the up- and downstream regions (+/– 50 Kb). Significance was determined using Mann-Whitney's test. **C**, Q-ChIP analysis of RNA polymerase II binding at the 5' and 3' regions of a subset of genes that were shown to be looped and upregulated in GCB-cells (ordered by degree of looping in GCB vs NB-cells), not looped and upregulated in GCB-cells, versus not looped and not upregulated in GCB-cells. Q-ChIP was performed in a GCB-cell line, OCI-Ly1. ChIP enrichment was calculated as the percentage of total chromatin (input) for each primer set and is expressed as the fold change in RNA polymerase II enrichment over the IgG control (to compare between biological replicates). The black dotted line indicates a fold change of 1.0 (no difference between RNA polymerase II enrichment and IgG control); the red dotted line indicates a 2-fold change in RNA polymerase II enrichment over the IgG control. The constitutively expressed *ACTB* gene (5' promoter region) was used as a positive control for RNA polymerase II binding; a gene desert region (*ENr313*) was used as a negative control.

Figure S3

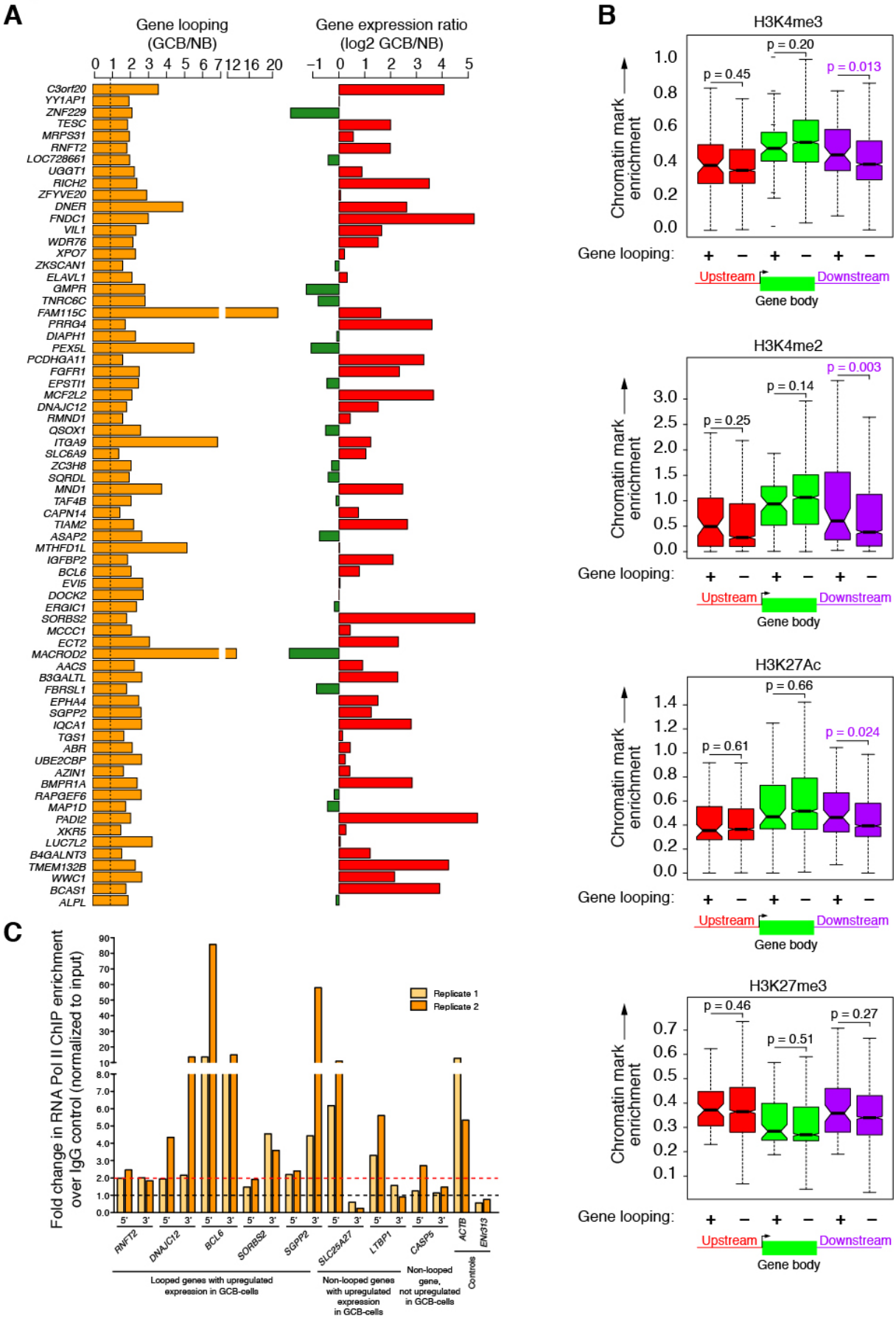
A
Gene looping (GCB/NB)
Gene expression ratio (log2 GCB/NB)
B
H3K4me3
H3K4me2
H3K27Ac
H3K27me3
Chromatin mark enrichment
Gene looping:
Upstream
Downstream
Gene body
p = 0.45
p = 0.20
p = 0.013
p = 0.25
p = 0.14
p = 0.003
p = 0.61
p = 0.66
p = 0.024
p = 0.46
p = 0.51
p = 0.27
C
Fold change in RNA Pol II ChIP enrichment over IgG control (normalized to input)
Replicate 1
Replicate 2
RNFT2
DNAJC12
BCL6
SORBS2
SGPP2
SLC25A27
LTBP1
CASP5
ACTB
EN313
Looped genes with upregulated expression in GCB-cells
Non-looped genes with upregulated expression in GCB-cells
Non-looped gene, not upregulated in GCB-cells
Controls

Figure S4. Formation of 3D gene neighborhoods in mature B-cells defines co-regulated gene units, which are remodeled in GCB-cells (related to Figure 4).

A, CTCF and RAD21 mark 3D gene neighborhoods in NB and GCB-cells. Degree of enrichment of CTCF or RAD21 binding at 3D gene neighborhood boundaries versus the whole genome in NB and GCB-cells. Asterisk indicates a significant increase in enrichment of these factors at boundaries compared to the genome ($p<10\text{-}9$, Mann-Whitney's test). **B**, Degree of coordinated gene expression and histone modifications within 3D gene neighborhoods (red) or among randomly selected genes (blue) in NB-cells. Significance was determined using Fisher's exact test. **C**, Schematic illustrating the role of interaction domains in the formation of co-regulated gene units (3D gene neighborhoods). Coordinate expression and chromatin status of genes within a 3D gene neighborhood are indicated by the color switch to red. **D**, Expansion of chromosomal territories associated with active chromatin in GCB-cells. Zoomed-out view of a region of chromosome 3 showing chromosome territories (as defined by PC1 of distance-normalized Pearson correlation matrix plots of Hi-C interactions at 1 Mb scale) versus gene density and H3K4me3 levels in NB and GCB-cells. Chromosome territories representing active chromatin compartments (positive PC1 values) are colored red, inactive chromatin compartments (negative PC1 values) are colored blue. The gene expression ratio between GCB and NB-cells is indicated below. Many active chromatin compartments within this region become expanded in GCB-cells (highlighted by orange shading) and contain genes that are up-regulated during GCB-cell differentiation, which are highlighted.

Figure S4

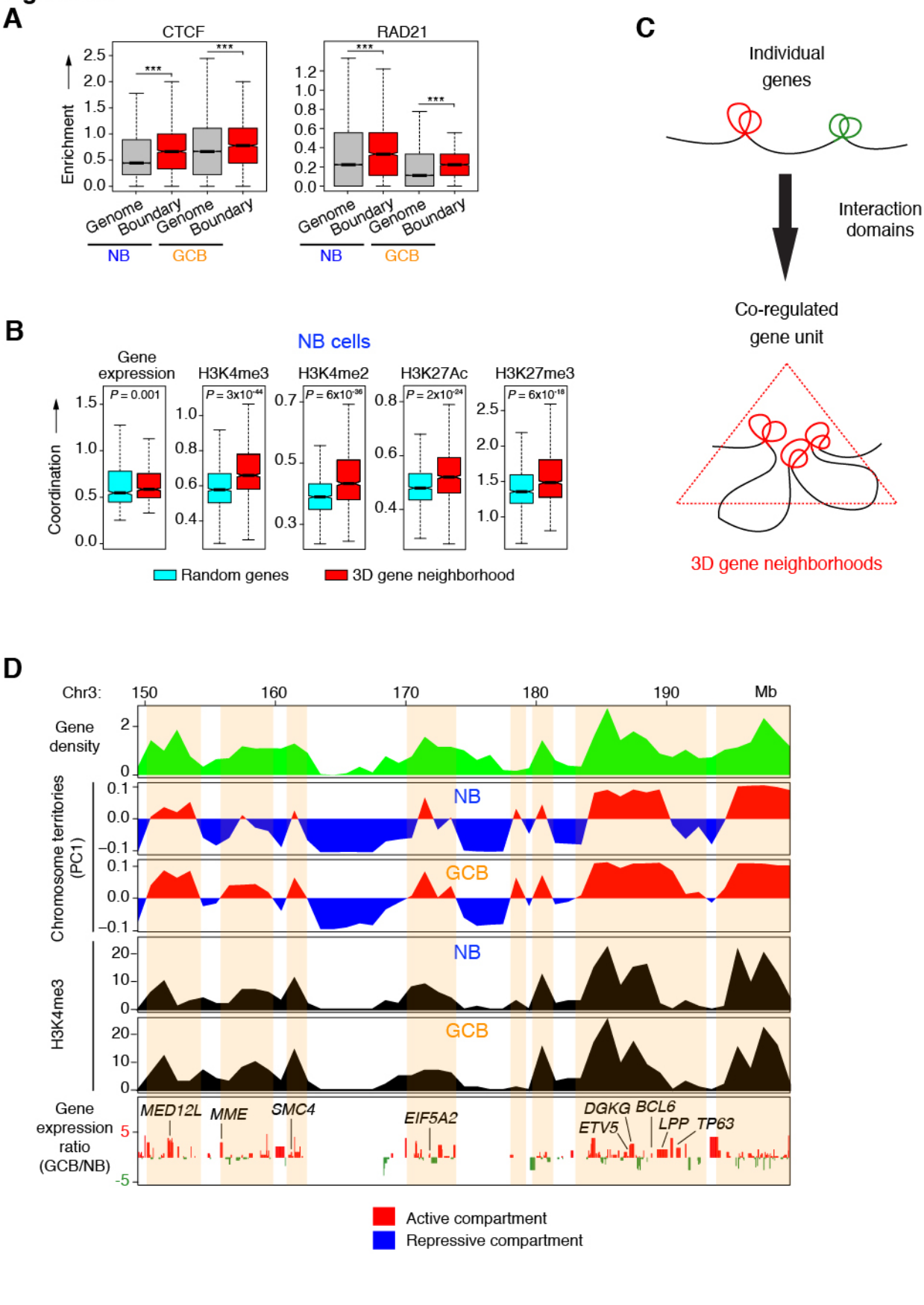
A
CTCF
RAD21
Enrichment
Genome
Boundary
NB
GCB
B
NB cells
Gene expression
H3K4me3
H3K4me2
H3K27Ac
H3K27me3
Coordination
Random genes
3D gene neighborhood
C
Individual genes
Interaction domains
Co-regulated gene unit
3D gene neighborhoods
D
Chr3:
Mb
Gene density
Chromosome territories (PC1)
H3K4me3
Gene expression ratio (GCB/NB)
MED12L
MME
SMC4
EIF5A2
DGKG
BCL6
ETV5
LPP
TP63
Active compartment
Repressive compartment

Figure S5. The *BCL6* promoter interacts with other GC signature genes (related to Figure 5).
A, Tracks showing normalized Hi-C interaction frequencies and normalized read counts of contacts made with the *BCL6* gene promoter (4C-seq anchor), as detected by 4C-seq, in NB and GCB-cells across the *BCL6* gene. Interactions between the *BCL6* promoter and 3' and downstream regions are higher in GCB-cells (highlighted). **B**, Gene set enrichment and depletion among genes that form a GCB-cell-specific interaction network with *BCL6*, with GC phenotype-driving genes listed.

Figure S5

A

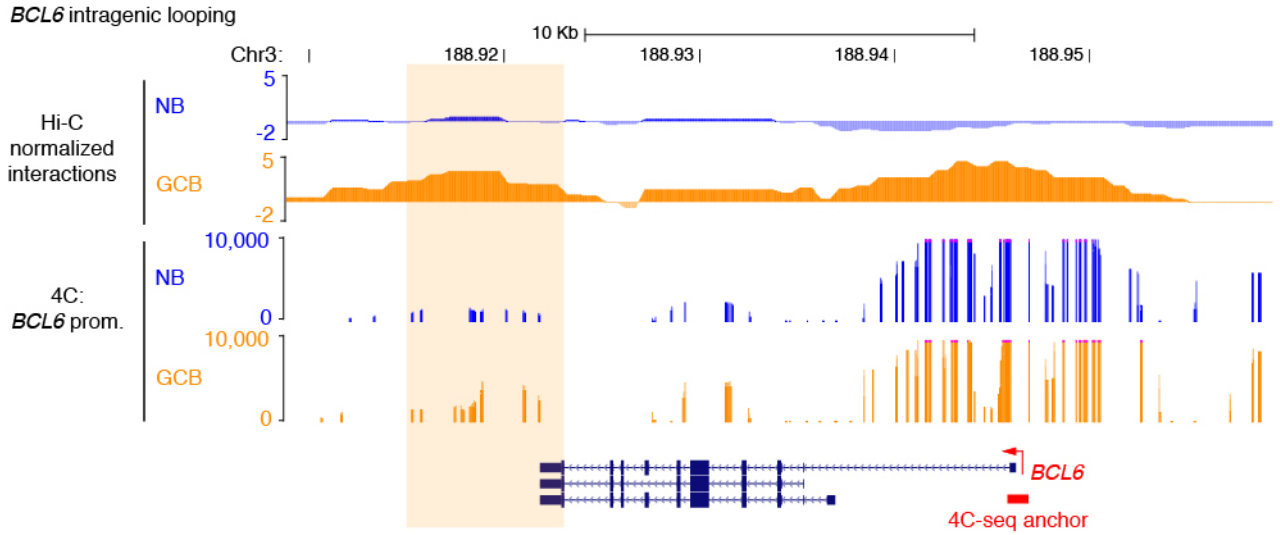
BCL6 intragenic looping
10 Kb
Chr3:
188.92
188.93
188.94
188.95
Hi-C normalized interactions
NB
GCB
5
-2
4C: BCL6 prom.
10,000
0
BCL6
4C-seq anchor

B

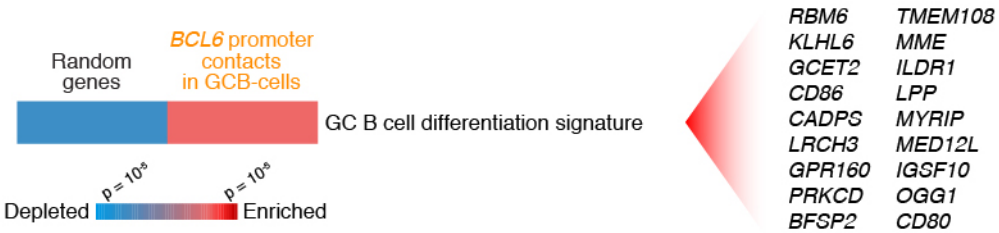
Random genes
BCL6 promoter contacts in GCB-cells
GC B cell differentiation signature
p = 10⁵
p = 10⁵
Depleted
Enriched
RBM6
KLHL6
GCET2
CD86
CADPS
LRCH3
GPR160
PRKCD
BFSP2
TMEM108
MME
ILDR1
LPP
MYRIP
MED12L
IGSF10
OGG1
CD80

Figure S6. Characterization of LCR-deficient mice (related to figure 7).

A, H3K27Ac read densities (normalized to input) from ChIP-seq data in human tissues focused around chr3:187457279-187875742 (human genome assembly 19). The putative locus control region is shaded in orange. Data from spleen, thymus, heart, lung and hippocampus were derived from publicly available datasets. **B-D**, Representative flow cytometry plots (left) of WT and LCR-deficient mice along with quantification (right) of (B) B220+, DAPI- B-cells, (C) B220+, DAPI-, CD38-, FAS+ GCB-cells and (D) B220-, CD3-, GR1+ and CD11b+ Monocytes. **E**, Representative images of BCL6 stained brain sections from the WT (left) and LCR-deficient (right) mice. Sc is subiculum (a region inferior to the hippocampus). Top to bottom, sequentially zoomed in images of the subiculum with normal BCL6 staining in both WT and LCR-deficient mice. **F**, Schematic of the LCR upstream of *Bcl6* in the murine genome (chr16) highlighting the genotyping strategy employing two PCRs. Genes are depicted in yellow boxes, LCR is depicted with a green box, dotted arrows indicate genomic distance in Kb. Solid black arrows indicate direction of transcription for respective genes whereas the blue and green solid arrows depict the PCR primers. **G**, Agarose gel images with PCR products stained with ethidium bromide. The 'PCR for deleted LCR' gives rise to a 70bp product if the LCR has been deleted in at least one of the homologous chromosomes indicating the possibility of an LCR-knock out or LCR-heterozygous mouse. 'PCR for LCR' gives rise to a 172bp product if the LCR is intact in one of the two homologous chromosomes. A mouse with a homozygous deletion of the LCR would have a 70bp product for the 'deleted LCR' reaction but no product in the 172 bp region for the second PCR (for LCR). **H**, Sequencing the PCR product from the 'deleted LCR' reaction reveals a part of the product from the left side of the LCR and the remaining part of the product from the right side of the LCR, thereby confirming the deletion of the ~165Kb region.

Data in B and C and are representative from one of two replicate experiments from independently created LCR-deficient mice. B and C are from the first cohort with 5 WT littermates and 4 LCR-deficient mice. Data in D is from the second independently generated cohort with 4 WT littermates and 5 LCR-deficient mice. Quantified data in B, C and D is shown as mean ± SEM. Significance is calculated by performing a two-tailed, unpaired t-test. P-values are listed wherever the difference is significant. Blue bars are for WT and red for LCR-deficient mice. n.s. is non significant. Monocytes flow plot and quantification (S6D) are from an independently created LCR-deficient cohort of mice.

Figure S6

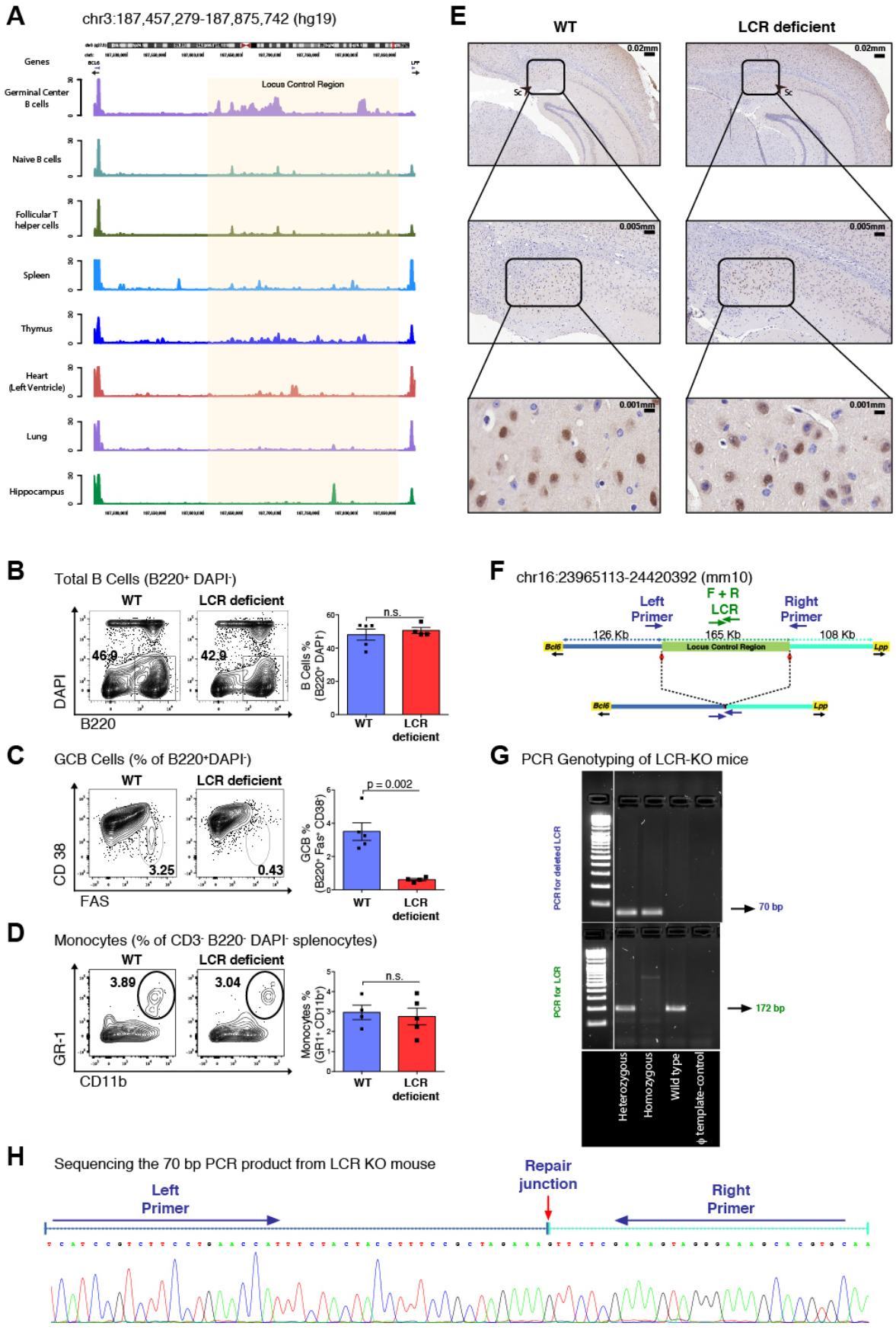
A
chr3:187,457,279-187,875,742 (hg19)
Genes
Locus Control Region
Germinal Center B cells
Naive B cells
Follicular T helper cells
Spleen
Thymus
Heart (Left Ventricle)
Lung
Hippocampus
E
WT
LCR deficient
0.02mm
0.005mm
0.001mm
Sc
B
Total B Cells (B220+ DAPI-)
WT
LCR deficient
46.9
42.9
DAPI
B220
n.s.
B Cells % (B220+ DAPI-)
C
GCB Cells (% of B220+DAPI-)
3.25
0.43
CD 38
FAS
p = 0.002
GCB % (B220+ Fas+ CD38-)
D
Monocytes (% of CD3- B220- DAPI- splenocytes)
3.89
3.04
GR-1
CD11b
Monocytes % (GR1+ CD11b+)
F
chr16:23965113-24420392 (mm10)
Left Primer
F + R LCR
Right Primer
126 Kb
165 Kb
108 Kb
Bcl6
Locus Control Region
Lpp
G
PCR Genotyping of LCR-KO mice
PCR for deleted LCR
PCR for LCR
70 bp
172 bp
Heterozygous
Homozygous
Wild type
ϕ template-control
H
Sequencing the 70 bp PCR product from LCR KO mouse
Left Primer
Repair junction
Right Primer

Supplemental Tables

Table S1. Summary of sequenced reads and filtered Hi-C interactions in NB and GCB-cells (related to Figure 1).
Table S2. Summary of sequenced reads, filtered and gained 4C intra-chromosomal interactions and overlap with genes in NB and GCB-cells (related to Figure 5).
Table S3. Primer sequences used for QChIP (related to Figure 3).
Table S4. Primer sequences used for *BCL6* 3C assays (related to Figure 2 and 3).
Table S5. Primer sequences used for *CKS2* 3C assays (related to Figure 2).
Table S6. Oligos and primers for LCR-deficient mouse generation and genotyping (related to Figure 7)**.**
Table S7. Primer sequences used for *BCL6* gene promoter and enhancer (LCR) 4C-seq library generation (related to Figure 5).

Table S1. Summary of sequenced reads and filtered Hi-C interactions in NB and GCB-cells.

Cell replicate	Number of uniquely aligned read-pairs	Number of intra-chromosomal interactions	Merged intra-chromosomal interactions*
NB replicate 1	142,592,815	76,154,185	146,279,288
NB replicate 2	164,792,135	79,983,990	
GCB replicate 1	200,106,474	47,894,791	60,524,352
GCB replicate 2	254,517,909	29,327,675	

*Merged = the union of the data (final set of interactions used).

Table S2. Summary of sequenced reads, filtered and gained 4C intra-chromosomal interactions and overlap with genes in NB and GCB-cells.

BCL6 bait sequence	Cell replicate	Number of uniquely aligned reads	Number of 4C interactions gained in GCB vs NB-cells (FDR=0.05)	Number of genes that overlap with gained 4C interactions in GCB-cells
BCL6 promoter	NB replicate 1	49,254,494		
	NB replicate 2	68,891,826		
	GCB replicate 1	70,686,806	3,307	583
	GCB replicate 2	67,552,953	3,011	563
BCL6 enhancer (LCR)	NB replicate 1	24,481,020		
	NB replicate 2	23,186,227		
	GCB replicate 1	28,689,104	2,344	494
	GCB replicate 2	25,546,152	2,983	619

Table S3. Primer sequences used for QChIP.

Primer name	Primer sequence (5'-3')
RNFT2 5' Forward	GCCAAGAAACCACCCAATAG
RNFT2 5' Reverse	CCCAGACAATTCAGCAATCA
RNFT2 3' Forward	AGAAAGGCAAGCTTTGGACA
RNFT2 3' Reverse	CCCGGATGTCTTCCTAACAC
DNAJC12 5' Forward	TCTTCCCTCGGAAACAAGAG
DNAJC12 5' Reverse	GCTATGTGGAACATGCTGCT
DNAJC12 3' Forward	TTCAAGGATGGAGGAATCAA
DNAJC12 3' Reverse	GCAAGACTGTCCCCTATGCT
BCL6 5' Forward	GGCAGCAACAGCAATAATCA
BCL6 5' Reverse	GCAGTGGTAAAGTCCGAAGC
BCL6 3' Forward	CAACGCGGTAATGCAGTTTA
BCL6 3' Reverse	TAGGCAGACACAGGGACTTG
SORBS2 5' Forward	CAGTCAACAGCCTGTCCAAA
SORBS2 5' Reverse	AGAGAAGCAATGGGCATGTT
SORBS2 3' Forward	AGAAGGCAGGCAACTCACAT
SORBS2 3' Reverse	GGAGGCTCAGCATTTCTGTT
SGPP2 5' Forward	GCCTTCCAGTAACCAGGATG
SGPP2 5' Reverse	GACTGCATTGAAAGCGTCTG
SGPP2 3' Forward	AGAACATCCCACCACTCACC
SGPP2 3' Reverse	AAGCTGACGAACCAAGAGGA
SLC25A27 5' Forward	GCGAGAAGGAGTGCGTTATC
SLC25A27 5' Reverse	AGCCGGACAGTAGGAATTTG
SLC25A27 3' Forward	CCCAAGTGTTCTGCATTGAA
SLC25A27 3' Reverse	CCGACCCCACAAAGAATAAA
LTBP1 5' Forward	CAAATGTGGTTTTGGAGTGC
LTBP1 5' Reverse	CAACCCGACAGGTTTAAGGA
LTBP1 3' Forward	ATCCCACTCTCCCCACTTTT
LTBP1 3' Reverse	TGTTAGGGGAAACAATTTAGCC
CASP5 5' Forward	CCAGCTGCTAGTCAGAAAAGG
CASP5 5' Reverse	TGAGTCTGAGGCACTTTCCA
CASP5 3' Forward	TTGTTGGCGGTAAGTCACAG
CASP5 3' Reverse	TCAATGAAAATGGTGGACGA
ACTB 5' Forward	GAACTGGCGTGGGGTGTC
ACTB 5' Reverse	AGCACAGAGCCTCGCCTTT
ENr313 Forward	CTGCTGCTGCTAATGCTGTC
ENr313 Reverse	CATGCTGACATAGGCAGGAA

Table S4. Primer sequences used for *BCL6* 3C assays.

Primer name	Primer sequence (5'-3')
BCL6 downstream 3	TGATTACAGTGGGTTCCGAAG
BCL6 downstream 2	GGAATGAGAGAAGGCCACTTT
BCL6 downstream 1	TTGGCCACTAACCATTCATAA
BCL6 gene 2	CGGAGCTAGAACCCATAAGAA
BCL6 gene 1	CTATCACGTTTCCTGCCAAC
BCL6 promoter 1	CCCTCAAGCGTTTTAAAGATGT
BCL6 promoter 2	GCCTTGGCTATGAGAGTCCTT
BCL6 promoter 3/upstream 1	CTGATCATTGCTGCTGGGTA
BCL6 intergenic 1	TCCAGTTGTGAAGTCTGTGCT
BCL6 intergenic 2	TATTCCATGGCACTTCATCG
BCL6 intergenic 3	CCTATAGGCCGAGATGCTGT
BCL6 intergenic 4	GCAAGGGAGCATTAAGGTTG
BCL6 intergenic 5	GGTCTTCAGGGAACAACTGG
BCL6 intergenic 6	TGGATGGTGGAGAGAAAGAAA
BCL6 enhancer 1A	AGAAAGGAAGGGGTCTCCAG
BCL6 enhancer 1B	CCATAAATGCCCAGCCTAGT
BCL6 enhancer 1C	AAGCAAGTGGGTAACATGGTC
BCL6 enhancer 1D	AAGTCGCGATCTTAACAATGG
BCL6 enhancer 1E	CGGAAAGATTAAACCTTATTCTATGA
BCL6 enhancer 1F	AATTCCAGCTGCACAATCTG
BCL6 enhancer 1G	GGGCAAGTTTGTAAACATCATT
BCL6 enhancer 1H	AGGTTGCCATGCTAGTTGCT
BCL6 enhancer 1I	TTGCAAGCATTGTGCTACCT
BCL6 enhancer 1J	GTGGGTCATTTGCCTCATCT
BCL6 enhancer 1K	CTCAGCAACTCTGCAAAACAG
BCL6 enhancer 1L	ATCAATTCCTCAAGGGAAGC
BCL6 enhancer 1M	AAAAATTTCCCCAGTTGAGGT
BCL6 enhancer 1N	CACTATGGTGGCTGTTGGAA
BCL6 enhancer 1O	TTCCTCTGGGGTTAGCTGAG
BCL6 enhancer 1P	CTCTTGTGAGTGGGGCTTTC
BCL6 enhancer 1Q	CTGGTTCTGGCCTATTGTGA
BCL6 enhancer 2A	AATGGACTGGCACATAAATGG
BCL6 enhancer 2B	CAGATCACAGTTGCTGAACCA
BCL6 enhancer 2C	AGGAGCACTGGTTAGCTGAAG
BCL6 enhancer 2D	TAGGCAGTGTTCCTCCCTTT
BCL6 enhancer 2E	TTATGTGGAAAGGCCAAAGG
BCL6 enhancer 2F	CCCCCTCCTTAATAACCCTAA
BCL6 enhancer 2G	AGCAAAGAAAAGTTCCATTTTAGTT
BCL6 enhancer 2H	GACTTATTGCCCAGCACACA
BCL6 enhancer 2I	CTGGCAGAGGTAAGGGATTG
BCL6 enhancer 2J	CATTTACCAGCTATGACCTTGG
BCL6 enhancer 2K	GCCAGGAGGCTTGTTAACTG

Table S5. Primer sequences used for *CKS2* 3C assays.

Primer name	Primer sequence (5'-3')
CKS2 upstream 1	GGTCCTATCCCAGACCAATG
CKS2 upstream 2	TGCTTTCTGGGATGATTTTG
CKS2 upstream 3	AGCATCAGGGCAAAGAGTTC
CKS2 promoter 1	GCAAGATGTAGGCCCAAGTT
CKS2 promoter 2	TCCCCTTATCCAGGAATTAGC
CKS2 promoter 3	TTTCTTGTTTTTGAAGTGAGTGG
SECISBP2 gene 1	GTGCATCTGTGCCAACTTGT
SECISBP2 gene 2	GACCATTGCTTCATCAGCAG
SECISBP2 gene 3	CAGATTTTGTTTTATTTTCCCAAGA
CKS1 Enhancer 1A	TTTCTTATCTCAGGGGTTTGC
CKS1 Enhancer 1B	GGAGGGAGCTACCTGCTCTT
CKS1 Enhancer 1C	TGGATCTGTCATCCACAAGC
CKS1 Enhancer 1D	GCCACTGATAGGAGGAGGTG
CKS1 Enhancer 1E	GCAGTAGCAAGAGCGAAAGAA
CKS2 Enhancer 2A	AATAAATTGGCCCAGCACAC
CKS2 Enhancer 2B	AGTCAAAGCTGGCCATTAGC
CKS2 Enhancer 2C	GTCACCCTCTTCCTCACCAG
CKS2 Enhancer 2D	TGCATACAGAAGAACATGAGAGAA
CKS2 Enhancer 2E	TAGTGGCATGCAGAGTGTCC
CKS2 Enhancer 2F	AATGGAGCAATTTGGTGGAC
CKS2 Enhancer 2G	GCCATCTGAGAAGTGCTGTG
CKS2 Enhancer 2H	TCCAGGTGGAGAGGTGACTT
CKS2 Enhancer 2I	CTGGGTGAATCTCTGCTCCT
CKS2 Enhancer 2J	GCACGCTTCTGCATTATTTG
CKS2 Enhancer 2K	AAGGCTGTGCTGTGCCTTAT

Table S6. Oligos and primers for LCR-deficient mouse generation and genotyping.

Primer name	Primer sequence (5'-3')	Purpose
mCr_BCL6enh_Tg1_1F	CACCGATTTTTGTGAGTACGGATT	CRISPR oligo for cloning in pX330
mCr_BCL6enh_Tg1_1R	AAACAATCCGTACTCACAAAAATC	CRISPR oligo for cloning in pX330
mCr_BCL6enh_Tg3_2F	CACCGTGTCAGCGACTCATAAGTTA	CRISPR oligo for cloning in pX330
mCr_BCL6enh_Tg3_2R	AAACTAACTTATGAGTCGCTGACAC	CRISPR oligo for cloning in pX330
TgSpBCL6enh_Tg1_1	TTAATACGACTCACTATAGCACCGATTTT TGTGAGTACGGATT	Forward primer for amplification of template for IVT of left sgRNA
TgSpBCL6enh_Tg3_2	TTAATACGACTCACTATAGCACCGTGTCA GCGACTCATAAGTTA	Forward primer for amplification of template for IVT of left sgRNA
T7-sgR_Rev	AAAAGCACCGACTCGGTGCC	Reverse primer for amplification of template for IVT of both sgRNA
For_Tg1_1_q	CATCCGTCTTCCTGAACCAT	Forward primer for genotyping product flanking LCR
Rev_Tg3_2_q	GCACGTGCTTTCCCTACTTT	Reverse primer for genotyping product flanking LCR
For_LCR1_1_q	GCTTGTGGACTTGCATCTCA	Forward primer for genotyping product within LCR
Rev_LCR1_1_q	TGTGGGTCTGTGTGTGAACAT	Reverse primer for genotyping product within LCR

Table S7. Primer sequences used for *BCL6* gene promoter and enhancer (LCR) 4C-seq library generation.

BCL6 promoter NlaIII reverse 4C-seq primer
CAAGCAGAAGACGGCATACGAGATAGGTGATTATTGCTGTTGCTG
BCL6 promoter HindIII forward 4C-seq primers
AATGATACGGCGACCACCGAGATCTACACTCTTTCCCTACACGACGCTCTTCCGATCTATCACGCAATACTAATACTATTGAAAGAAGCTT
AATGATACGGCGACCACCGAGATCTACACTCTTTCCCTACACGACGCTCTTCCGATCTCGATGTCAATACTAATACTATTGAAAGAAGCTT
AATGATACGGCGACCACCGAGATCTACACTCTTTCCCTACACGACGCTCTTCCGATCTTTAGGCCAATACTAATACTATTGAAAGAAGCTT
AATGATACGGCGACCACCGAGATCTACACTCTTTCCCTACACGACGCTCTTCCGATCTTGACCACAATACTAATACTATTGAAAGAAGCTT
AATGATACGGCGACCACCGAGATCTACACTCTTTCCCTACACGACGCTCTTCCGATCTACAGTGCAATACTAATACTATTGAAAGAAGCTT
AATGATACGGCGACCACCGAGATCTACACTCTTTCCCTACACGACGCTCTTCCGATCTGCCAATCAATACTAATACTATTGAAAGAAGCTT
AATGATACGGCGACCACCGAGATCTACACTCTTTCCCTACACGACGCTCTTCCGATCTCAGATCCAATACTAATACTATTGAAAGAAGCTT
AATGATACGGCGACCACCGAGATCTACACTCTTTCCCTACACGACGCTCTTCCGATCTACTTGACAATACTAATACTATTGAAAGAAGCTT
AATGATACGGCGACCACCGAGATCTACACTCTTTCCCTACACGACGCTCTTCCGATCTGATCAGCAATACTAATACTATTGAAAGAAGCTT
AATGATACGGCGACCACCGAGATCTACACTCTTTCCCTACACGACGCTCTTCCGATCTTAGCTTCAATACTAATACTATTGAAAGAAGCTT
AATGATACGGCGACCACCGAGATCTACACTCTTTCCCTACACGACGCTCTTCCGATCTGGCTACCAATACTAATACTATTGAAAGAAGCTT
AATGATACGGCGACCACCGAGATCTACACTCTTTCCCTACACGACGCTCTTCCGATCTATGTCACAATACTAATACTATTGAAAGAAGCTT
AATGATACGGCGACCACCGAGATCTACACTCTTTCCCTACACGACGCTCTTCCGATCTCCGTCCCAATACTAATACTATTGAAAGAAGCTT
AATGATACGGCGACCACCGAGATCTACACTCTTTCCCTACACGACGCTCTTCCGATCTGTCCGCCAATACTAATACTATTGAAAGAAGCTT
AATGATACGGCGACCACCGAGATCTACACTCTTTCCCTACACGACGCTCTTCCGATCTGAGTGGCAATACTAATACTATTGAAAGAAGCTT
AATGATACGGCGACCACCGAGATCTACACTCTTTCCCTACACGACGCTCTTCCGATCTATTCCTCAATACTAATACTATTGAAAGAAGCTT
BCL6 enhancer NlaIII reverse 4C-seq primer
CAAGCAGAAGACGGCATACGAGATCCTCACAATCCTCTCATCTTCAAAG
BCL6 enhancer HindIII forward 4C-seq primer
AATGATACGGCGACCACCGAGATCTACACTCTTTCCCTACACGACGCTCTTCCGATCTATCACGCTGTCTAAATATTCCAAAGCCAAGCTT
AATGATACGGCGACCACCGAGATCTACACTCTTTCCCTACACGACGCTCTTCCGATCTCGATGTCTGTCTAAATATTCCAAAGCCAAGCTT
AATGATACGGCGACCACCGAGATCTACACTCTTTCCCTACACGACGCTCTTCCGATCTTTAGGCCTGTCTAAATATTCCAAAGCCAAGCTT
AATGATACGGCGACCACCGAGATCTACACTCTTTCCCTACACGACGCTCTTCCGATCTTGACCACTGTCTAAATATTCCAAAGCCAAGCTT
AATGATACGGCGACCACCGAGATCTACACTCTTTCCCTACACGACGCTCTTCCGATCTACAGTGCTGTCTAAATATTCCAAAGCCAAGCTT
AATGATACGGCGACCACCGAGATCTACACTCTTTCCCTACACGACGCTCTTCCGATCTGCCAATCTGTCTAAATATTCCAAAGCCAAGCTT
AATGATACGGCGACCACCGAGATCTACACTCTTTCCCTACACGACGCTCTTCCGATCTCAGATCCTGTCTAAATATTCCAAAGCCAAGCTT
AATGATACGGCGACCACCGAGATCTACACTCTTTCCCTACACGACGCTCTTCCGATCTACTTGACTGTCTAAATATTCCAAAGCCAAGCTT
AATGATACGGCGACCACCGAGATCTACACTCTTTCCCTACACGACGCTCTTCCGATCTGATCAGCTGTCTAAATATTCCAAAGCCAAGCTT
AATGATACGGCGACCACCGAGATCTACACTCTTTCCCTACACGACGCTCTTCCGATCTTAGCTTCTGTCTAAATATTCCAAAGCCAAGCTT
AATGATACGGCGACCACCGAGATCTACACTCTTTCCCTACACGACGCTCTTCCGATCTGGCTACCTGTCTAAATATTCCAAAGCCAAGCTT
AATGATACGGCGACCACCGAGATCTACACTCTTTCCCTACACGACGCTCTTCCGATCTATGTCACTGTCTAAATATTCCAAAGCCAAGCTT
AATGATACGGCGACCACCGAGATCTACACTCTTTCCCTACACGACGCTCTTCCGATCTCCGTCCCTGTCTAAATATTCCAAAGCCAAGCTT
AATGATACGGCGACCACCGAGATCTACACTCTTTCCCTACACGACGCTCTTCCGATCTGTCCGCCTGTCTAAATATTCCAAAGCCAAGCTT
AATGATACGGCGACCACCGAGATCTACACTCTTTCCCTACACGACGCTCTTCCGATCTGAGTGGCTGTCTAAATATTCCAAAGCCAAGCTT
AATGATACGGCGACCACCGAGATCTACACTCTTTCCCTACACGACGCTCTTCCGATCTATTCCTCTGTCTAAATATTCCAAAGCCAAGCTT

Supplemental Experimental Procedures

Bioinformatics analysis

Hi-C data showed an expected inverse correlation between interaction frequency and distance (**Figure S1D**). Hi-C reads connecting non-overlapping 1 Mb windows were counted to generate genome-wide contact matrices. Spearman correlation of contact matrices between biological replicates was used to assess reproducibility. Correlation heat-maps were generated (Lieberman-Aiden et al., 2009) and principal component analysis (PCA) performed to identify first eigenvectors that revealed local and global compartmentalization. Interaction frequency was defined as the total number of Hi-C reads involved in each 1 Kb genomic window, normalized by the total Hi-C read sequencing coverage for each chromosome in each sample. Since the presence of HindIII sites strongly influences the detection of Hi-C products, a regression model was used to subtract the number of interactions explainable by HindIII availability. Normalized interaction frequency was used for all subsequent integrative analyses, unless otherwise stated. Based on the number of intra-chromosomal interactions identified in naïve B and GCB-cells (**Table S1**), and correcting for hg18 genome mappability and the number of HindIII sites across each chromosome, the average 3D interaction counts per HindIII site are 346.33 for naïve B-cells and 143.30 for GCB-cells. When averaged across 1 kilobase-pair (Kb) mappable genomic windows, the 3D interaction counts are 114.38 for naïve B-cells and 47.33 for GCB-cells. This difference in read counts can be explained by the difference in the total numbers of reads that were sequenced in naïve B and GCB-cells. These counts are comparable to other published Hi-C data in human cells (Dixon et al., 2012), which, when filtered with our own stringent filtering criteria, achieved average 3D interaction counts (across 1 Kb windows) of 84.09 and 82.99, in ESCs and IMR90 cells, respectively. Interaction frequency for each gene was calculated at 20 equally spaced locations across the gene body and across the ± 50 Kb regions. A genome-wide interaction profile was generated by taking the average of all genes longer than 20 Kb. Differences in gene expression (RPKM) between naïve B and GCB-cells were calculated as the normalized log2 ratio of RPKM in GCB versus naïve B-cells. Gene Set Enrichment Analysis (GSEA) was performed by ranking genes by interaction frequency and using default parameters (Subramanian et al., 2005) with gene sets obtained from a curated database of normal and pathological lymphoid biology gene signatures (Shaffer et al., 2006). PCA was performed on genomic features of interest, with representative genes of each component defined as those with PCA scores ≥ 1 or ≤ -1. PCA scores were used to perform GSEA. Enhancers were defined as genomic regions marked by the presence of H3K4me2 ChIP-seq peaks, and by the absence of H3K4me3 ChIP-seq peaks ($H3K4me2^{pos}H3K4me3^{neg}$) in naïve B and GCB-cells, as defined in (Creyghton et al., 2010; Heintzman et al., 2007) and reviewed in (Ong and Corces, 2011). H3K4me2 and H3K4me3 ChIP-seq peaks were called at the following threshold (T) and fold change of ChIP signal compared to input (F) using our own algorithm, ChIPseeqer (Giannopoulou and Elemento, 2011): **H3K4me2:** T=15; F=2 and **H3K4me3:** T=5; F=2. Naïve B and GCB-cell-specific enhancers were defined as regions marked by $H3K4me2^{pos}H3K4me3^{neg}$ (as defined above), linked to genes <50 Kb away (5,167 and 5,339, respectively). Active enhancers were defined by the presence of H3K27Ac. For enhancer-promoter interactions, a combined set of 33,060 naïve B and GCB-cell enhancers ($H3K4me2^{pos}H3K4me3^{neg}$) was used. Using genes (1,832) that had differential expression between naïve B and GCB-cells, as measured by RNA-seq (FDR=0.05; (Wang et al., 2012)), we counted the number of Hi-C reads in naïve B-cells and GCB-cells connecting each gene promoter (gene TSS surrounded by a 5 Kb window) to all putative enhancers (regions defined as $H3K4me2^{pos}H3K4me3^{neg}$ surrounded by a 5 Kb window) within 1 Mb of each gene, as well as the total reads that overlap with the promoter region. Significant differences were identified using Fisher's exact tests with FDR control. Pathway Analysis of Gene Expression (iPAGE; (Goodarzi et al., 2009)) was used to investigate enrichment of gene sets among genes linked to naïve B- and GCB-specific enhancers and for genes residing within "3D gene cities" (see below). To test for gene body looping, Hi-C reads connecting the upstream and downstream 50 Kb regions of genes longer than 20 Kb were counted in naïve B and GCB-cells, respectively. Fisher's exact test with FDR control was performed to quantify looping changes; taking into account reads covering the upstream or downstream regions. The average read density of factors or histone marks was calculated at RefSeq gene promoters (± 2 Kb), enhancers ($H3K4me2^{pos}H3K4me3^{neg}$), and either the upstream, gene body, or downstream regions of RefSeq genes. Publicly available data were used for genome-wide binding of SPIB (HBL-1 cells) (Yang et al., 2012) and IRF8 (OCI-Ly1 cells) (Shin et al., 2011). Topological domains or "3D gene neighborhoods" were identified at a 100 Kb resolution (Dixon et al., 2012), using a three-state Hidden Markov Model with Gaussian emission probabilities, and directionality indices calculated on 4 Mb genomic windows. To determine enrichment of genomic features at topological boundaries, CTCF and RAD21 binding were calculated at boundaries and compared with their genome-wide binding using Mann-Whitney's test. As co-regulated genes tend to have similar patterns of gene expression, the score of expression co-regulation S_{coreg} was defined for a set of genes as: $S_{coreg}(G) = \frac{1}{stdev(G)}$ where G are the log2 RPKM values of a set of n genes of interest and *stdev* denotes standard deviation. Higher S_{coreg} indicates tighter co-regulation and vice versa. This equation was also used to investigate histone mark concordance, using the log2 read density of genes as G. To determine whether genes in the same 3D gene neighborhood are co-regulated, for each 3D domain D_k, the co-regulation score S_{coreg_domain} for its n_k genes and S_{coreg_random} for n_k random genes was calculated. The genome-wide difference between S_{coreg_domain} and S_{coreg_random} was calculated using Mann-Whitney's test. The ratio of normalized reads between 3D gene neighborhoods in GCB versus naïve B-cells was used to define the formation of "3D gene cities". The ratio of reads connecting all neighboring domains larger than 500 Kb was calculated and compared with the respective changes of S_{coreg} in GCB versus naïve B-cells using the Spearman correlation.

Significant differences in 4C-seq read counts between GCB and naïve B-cells across chromosome 3 were calculated for 20 Kb chromosomal bins using an in-house algorithm and Fisher's exact test with Bonferroni correction (FDR=0.05). "Virtual 4C" was used to extract all contacts made with the *BCL6* gene promoter from the Hi-C data. Pearson correlation scores between the *BCL6* gene promoter contacts identified by virtual 4C (Hi-C data) compared with 4C-seq showed reproducibility between the two platforms: 0.58 in naïve B-cells and 0.74 in GCB-cells. *BCL6* promoter or enhancer 4C-seq contacts that were significantly gained in GCB-cells (compared to naïve B-cells) and overlapped with genomic regions encoding RefSeq genes (2 Kb upstream of the transcription start site (TSS) and 2 Kb downstream of the transcription termination site (TTS)), were used as input for iPAGE analysis. To examine overlap between *BCL6* enhancer 4C-seq contacts significantly gained in GCB-cells and other GCB-specific enhancers on chromosome 3, a subset of 991 enhancers ($H3K4me3^{neg}$ $H3K4me2^{pos}$) unique to GCB-cells (and not naïve B-cells) were used (from the 21,807 total enhancers identified in GCB-cells). Genes < 50Kb away from these overlapping GCB-specific enhancers were used as input for iPAGE analysis. GSEA was performed using the ranked list of 1,832 genes with significantly different expression in GCB versus naïve B-cells, and default settings.

Mouse genotyping

Genomic DNA was isolated from the 15 pups using the Viagen direct PCR (tail) lysis reagent (Cat#102-T), isopropanol precipitation and ethanol purification. Genotyping the LCR-deficient mice required two independent PCR reactions for each mouse (**Figure S6F and G**). Deletion of the LCR in at least one of the two homologous chromosomes was confirmed by the presence of a PCR product from a primer pair that flanked the LCR (**Table S6**). The second PCR confirmed the deletion of LCR in homologous chromosomes with a primer pair complementary to a region within the deleted LCR (**Table S6**). PCR with these primers revealed 3 of the 15 pups to have a deletion. The LCR deletion was further confirmed by sequencing the PCR product from the '*PCR for deleted LCR*' reaction. This involved cloning the 70bp product into a TOPO-TA vector, sequencing (Genewiz) and alignment of the sequence to the mouse genome. Mice with a deleted LCR gave rise to a product with a part of the sequence from left side of the LCR and the remaining part from the right side of the LCR (**Figure S6H**).

Supplemental References

Creyghton, M.P., Cheng, A.W., Welstead, G.G., Kooistra, T., Carey, B.W., Steine, E.J., Hanna, J., Lodato, M.A., Frampton, G.M., Sharp, P.A., et al. (2010). Histone H3K27ac separates active from poised enhancers and predicts developmental state. Proc Natl Acad Sci USA 107, 21931-21936.

Goodarzi, H., Elemento, O., and Tavazoie, S. (2009). Revealing global regulatory perturbations across human cancers. Molecular Cell *36*, 900-911.

Heintzman, N. D. *et al*. (2007). Distinct and predictive chromatin signatures of transcriptional promoters and enhancers in the human genome. *Nat. Genet.* **39**, 311–318.

Ong, C.-T. & Corces, V. G. (2014) CTCF: an architectural protein bridging genome topology and function. *Nat. Rev. Genet.* **15**, 234–246.

Shaffer, A.L., Wright, G., Yang, L., Powell, J., Ngo, V., Lamy, L., Lam, L.T., Davis, R.E., and Staudt, L. (2006). A library of gene expression signatures to illuminate normal and pathological lymphoid biology. Immunol Rev *210*, 67-85.

Shin, D.M., Lee, C., and Morse, H.C. (2011). IRF8 governs expression of genes involved in innate and adaptive immunity in human and mouse germinal center B cells. PLoS ONE *6*, e27384.

Subramanian, A., Tamayo, P., Mootha, V.K., Mukherjee, S., Ebert, B.L., Gillette, M.A., Paulovich, A., Pomeroy, S.L., Golub, T.R., Lander, E.S.*, et al.* (2005). Gene set enrichment analysis: a knowledge-based approach for interpreting genome-wide expression profiles. Proc Natl Acad Sci USA *102*, 15545-15550.

Yang, Y., Shaffer, A.L., Emre, N.C., Ceribelli, M., Zhang, M., Wright, G., Xiao, W., Powell, J., Platig, J., Kohlhammer, H.*, et al.* (2012). Exploiting Synthetic Lethality for the Therapy of ABC Diffuse Large B Cell Lymphoma. Cancer Cell *21*, 723-737.